Hückel versus Möbius aromaticity: The particle in a cylinder versus a Möbius strip

Evangelos Miliordos*

Laboratory of Physical Chemistry, Department of Chemistry, National and Kapodistrian University of Athens, P. O. Box 64 004, 15710 Zografou, Athens, Greece

(Received 22 October 2010; published 28 December 2010)

The one-particle-constrained-to-a-Möbius-strip model is studied quantum mechanically. The results are used to account for the chemical concept of Möbius aromaticity. In addition, the one-particle-in-a-cylinder model is used to explain the Hückel aromaticity. Using the principles of quantum mechanics and applying the appropriate boundary conditions, the $4N + 2$ and $4N$ electrons aromaticity rules are confirmed for these two types of aromaticity. A numerical technique for obtaining an exact solution of the Schrödinger equation of the Möbius model is also suggested.

DOI: 10.1103/PhysRevA.82.062118 PACS number(s): 03.65.Ge, 71.20.Rv

I. INTRODUCTION

Aromaticity is a well-embedded concept in organic chemistry. Its definition is included in almost any organic chemistry textbook (see, for instance, Ref. [1]). Any planar cyclic molecule with $4N + 2$ or $4N$ (N being positive integer) π-conjugated electrons is called aromatic or antiaromatic, respectively. The pattern aromatic molecule is benzene (C_6H_6) with six π electrons (see Sec. II), whereas an antiaromatic molecule is cyclobutadiene (C_4H_4) with four π electrons. This type of aromaticity is called Hückel aromaticity [1]. The reasons that the aromatic (or antiaromatic) compounds constitute a separate category may be epitomized to their "peculiar" chemical activity, their remarkable stability (or reactivity), and the induction of chemical shifts in nuclear magnetic resonance (NMR) experiments [2,3].

The Möbius strip (Fig. 1) appeared in the literature one and a half century ago. Independently, A. F. Möbius and J. B. Listing studied the properties of the one-sided, thus nonorientable, Möbius surface [4]. Practically, a Möbius strip can be formed by cutting a cylinder band or a holey disk, twisting the one edge by 180° and reattaching the two edges. In the past decade, Möbius-like molecules, such as annulenes, have gained considerable attention [5,6]. Indeed the topology (Möbius or ringlike) may depend on the solvent [7,8] or on the protonation degree [9]. In 1964 Heilbronner, using the Hückel theory, predicted, although did not state explicitly, that the aromaticity of a Möbius-like molecule obeys to the rule of $4N$ electrons (Möbius aromaticity) [10], as contrasted to the $4N + 2$ electrons rule of the Hückel aromaticity of a ringlike molecule. Whether the Möbius aromaticity is observed is of much debate (see Ref. [6] and references therein), while Heilbronner's results have recently been criticized [6].

Presently, the explanation of Hückel and Möbius aromaticities is attempted, based on the simplest possible models, the particle in a cylinder or the particle in a Möbius strip, respectively.

II. HÜCKEL AROMATICITY

Consider the molecule of benzene; all its 12 nuclei lie on a plane and six p_π atomic orbitals are perpendicular to this plane, forming a cylinder (see Fig. 2). This picture is reduced to the simplest one, one particle "moving" on this cylinder. To describe this model, the angle ϕ and distance s are defined, as depicted in Fig. 2(b). Angle ϕ runs between 0 and 2π radians and s between $-L/2$ and $L/2$ (L is the width of the cylinder). The Schrödinger equation in cylindrical coordinates with constant radius reads:

$$\hat{H}\Psi(s,\phi) = -\frac{\hbar^2}{2\mu}\left[\frac{\partial^2}{\partial s^2} + \frac{1}{R^2}\frac{\partial^2}{\partial \phi^2}\right]\Psi(s,\phi) = E\Psi(s,\phi), \quad (1)$$

where μ is the mass of the particle and R the radius of the cylinder. The solution is straightforward:

$$\Psi_{n,m}(s,\phi) = \sqrt{\frac{1}{\pi L}}\sin\left[\frac{n\pi}{L}\left(s + \frac{L}{2}\right)\right]e^{im\phi} \quad (2)$$

and

$$E_{n,m} = \frac{h^2}{8\mu L^2}n^2 + \frac{\hbar^2}{2\mu R^2}m^2, \qquad n = 1,2,\ldots, \text{and}$$
$$m = 0,\pm1,\pm2,\ldots \quad (3)$$

since $\Psi(-L/2,\phi) = \Psi(L/2,\phi) = 0$ is needed and $\Psi(s,\phi)$ should be single valued at any spatial point (x,y,z) or $\Psi(s,\phi + 2\pi) = \Psi(s,\phi)$.

Note that the p_π system of benzene can be described only by even values of n, since p_π orbitals are odd functions of s (they have node at $s = 0$). Indeed, for a p_π system consisting of $2p$ orbitals, $n = 2$ best matches, since no other node exists. The energy-level diagram with respect to m is given in Fig. 3. The energy levels are filled with noninteracting electrons, bearing in mind that according to Pauli's exclusion principle each level can host up to two electrons (Fig. 3). The fact that in the case of $4N + 2$ electrons the system is closed shell guarantees its stability, since reaction with other molecules would demand intramolecular electron spin decoupling and intermolecular recoupling, an energetically unfavorable process in most of the times, involving highly excited states. In addition, the induced diamagnetic electronic current evokes the observed chemical shift in the proton NMR experiments (aromaticity) [1]. On the other hand, the half-filled occasion of $4N$ electrons is called

*emiliord@chem.uoa.gr

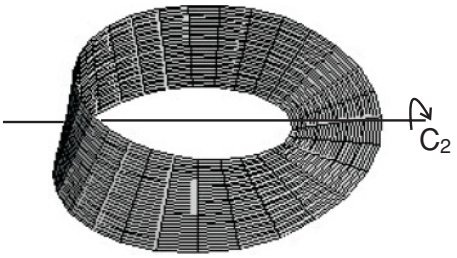

FIG. 1. The Möbius one-sided strip. Observe the C_2 axis of symmetry.

antiaromatic, and the paramagnetic now current causes the opposite chemical shift [3,11].

III. MÖBIUS AROMATICITY

Mathematically, the Möbius surface is called a ruled surface, since there is always a straight line passing from any of its points. This becomes clear if we construct the Möbius surface by rotating a stick of length L around two axes. We should revolve its center around an axis, say the z axis, drawing a circle of radius R, and simultaneously around an axis (υ axis) tangential to the previous circle. The stick remains always perpendicular to the υ axis (see Figs. 4 and 5). Instead of a circle, any arbitrary closed curve, called a median, can be used. The one-particle problem confined to a rather complicated Möbius-like strip has been studied earlier, inserting the Laplace-Beltrami operator in the Hamiltonian [12].

Next, the case of one-particle confined on a Möbius strip is studied. The "internal" coordinates of the problem, analogous to s and ϕ of Sec. II, are to be defined. Angles θ and ϕ correlate to the aforementioned rotations, while s is the distance of every point from the circular median line. In order to create a Möbius surface, we should demand $\phi = \pm 2\theta$, so after rotation of $\phi = 2\pi$ the stick can complete a half clockwise or counterclockwise twist ($\theta = \pm\pi$), while s takes values between $-L/2$ and $L/2$ (see Fig. 5). The two produced surfaces (choosing the

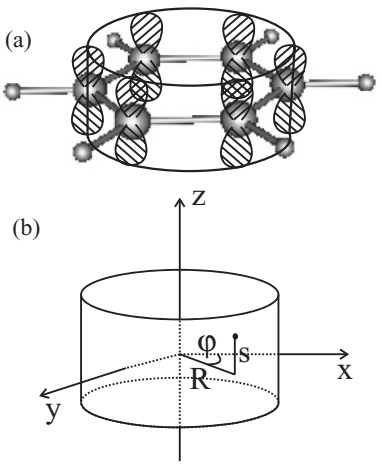

FIG. 2. (a) The π system of benzene. One electron in the benzene can be modeled as a particle constrained to the surface of a cylinder. (b) The surface of the cylinder can be described by s and ϕ (R is constant).

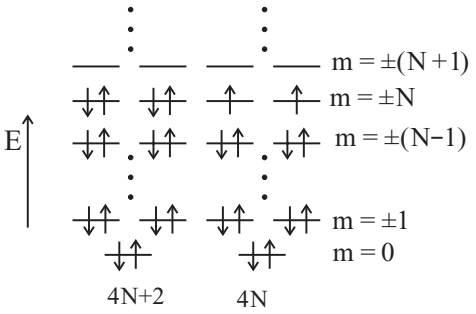

FIG. 3. Diagram of the first $2N + 3$ energy levels [$|m| = 0$–$(N+1)$] of the cylinder model occupied with $4N$ and $4N+2$ electrons. Energies of the levels are not in scale.

plus or minus sign) are mirror images of each other (see Fig. 6). Applying simple geometry and with the help of Fig. 5, the Cartesian coordinates, as a function of ϕ, $\theta = \phi/2$, and s are:

$$\begin{aligned} x &= (R + s\cos\theta)\cos\phi \\ y &= (R + s\cos\theta)\sin\phi \\ z &= s\sin\theta, \end{aligned} \tag{4}$$

consistent with those existing in the literature [13].

The Hamiltonian operator of both enantiomers in terms of ϕ and s is (see Appendix):

$$\hat{H} = -\frac{\hbar^2}{2\mu}\nabla^2 = -\frac{\hbar^2}{2\mu r}\left[\frac{\partial}{\partial s} r \frac{\partial}{\partial s} + \frac{\partial}{\partial \phi}\frac{1}{r}\frac{\partial}{\partial \phi}\right], \tag{5}$$

where $r = R + s\cos(\phi/2)$. Observe that the Hamiltonian commutes with the parity operator $\hat{P}_\phi$ ($\phi \to -\phi$), but it does not commute with either $\hat{P}_s$ ($s \to -s$) or $\hat{L}_z = \frac{\hbar}{i}\frac{\partial}{\partial\phi}$. The C_2 axis is along the x axis (see Figs. 1 and 5) and thus inverts the sign of y and z coordinates. Indeed, due to Eq. (4) its action is equivalent to $\hat{P}_\phi$. Toward the limit $R \gg L$ ($r \approx R$) one gets:

$$\hat{H} = -\frac{\hbar^2}{2\mu}\frac{\partial^2}{\partial s^2} - \frac{\hbar^2}{2\mu R^2}\frac{\partial^2}{\partial \phi^2}. \tag{6}$$

Now, $\hat{H}$ becomes separable and commutes with $\hat{P}_\phi$, $\hat{P}_s$, and $\hat{L}_z$. Applying $\Psi_{n,m}(-\frac{L}{2},\phi) = \Psi_{n,m}(\frac{L}{2},\phi) = 0$ for any ϕ, the normalized solution is

$$\Psi_{n,m}(s,\phi) = \sqrt{\frac{1}{\pi L}}\sin\left[\left(\frac{n\pi}{L}\left(s + \frac{L}{2}\right)\right)\right] e^{im\phi} \tag{7}$$

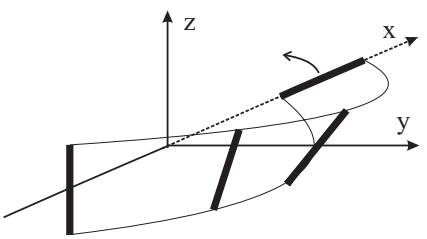

FIG. 4. The first half of the Möbius strip as formed according to the text.

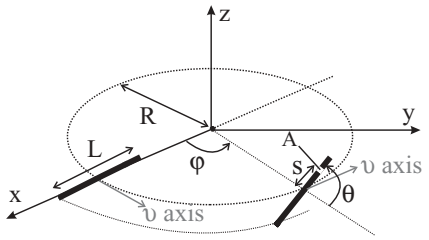

FIG. 5. The stick of length L is rotating around the variable υ axis, while its center draws a circle of radius R around the z axis. Any point A on the formed surface can be pinpointed using the parameters ϕ, θ, and s.

and

$$E_{n,m} = \frac{h^2}{8\mu L^2}n^2 + \frac{\hbar^2}{2\mu R^2}m^2, \quad n = 1,2,\ldots. \tag{8}$$

The allowed m values will be obtained after imposing the appropriate periodic constraint in $\Psi(s,\phi)$. According to Eq. (4) and $\phi = 2\theta$, observe that the $\phi \to \phi + 2\pi$, $s \to -s$ translation gives the same (x,y,z) coordinates. Demanding the eigenfunction to be single valued at each (x,y,z) point, it is equivalent to write

$$\Psi(-s,\phi + 2\pi) = \Psi(s,\phi). \tag{9}$$

Combining Eqs. (7) and (9) we have

$$\begin{aligned} &\text{for } n = \text{odd} \to m = 0, \pm 1, \pm 2, \ldots \\ &\text{for } n = \text{even} \to m = \pm\tfrac{1}{2}, \pm\tfrac{3}{2}, \ldots \end{aligned} \tag{10}$$

Of course, after a "full" rotation ($\Delta\phi = 4\pi$) Eq. (10) gives

$$\Psi(s,\phi + 4\pi) = \Psi(-s,\phi + 2\pi) = \Psi(s,\phi). \tag{11}$$

It is worthwhile to emphasize that this model shows the existence of half-integer orbital angular momentum ($L_z = \pm\frac{1}{2}\hbar, \pm\frac{3}{2}\hbar \ldots$ if n is even).

A last comment is in order: The Hamiltonian operators of the particle in a cylinder and that in a Möbius strip with $R \gg L$ are identical [see Eqs. (1) and (6)]. However, the nature of their solutions differs, clearly due to the different boundary conditions.

We turn, now, to the case of a molecule with Möbius conformation. All its atoms, forming the σ skeleton of the molecule, lie on the Möbius strip. Its p_π system, orthogonal to the σ-bonding backbone, forms as well a new Möbius strip perpendicular to that of the molecule (see Fig. 7). Since the p_π system, lying on the new Möbius strip, is related to $n = 2$ (see Sec. II), m can be only a half-integer, and the energy-level diagram of the π system is shown in Fig. 8. Consequently, the aromaticity rule is inverted: the $4N$ electron system is aromatic, whereas the $4N + 2$ electron system is antiaromatic.

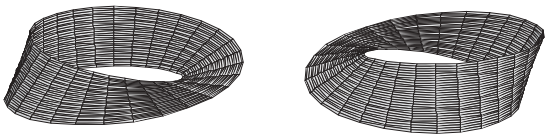

FIG. 6. Two chiral Möbius surfaces.

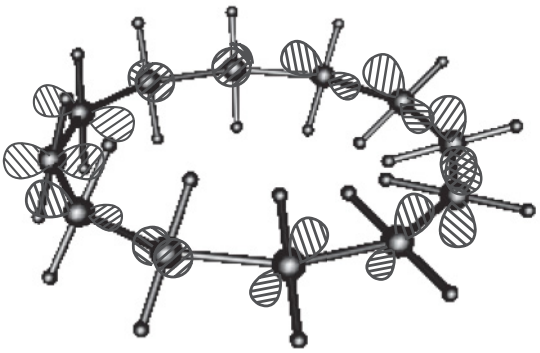

FIG. 7. The σ (atoms and bonds represented by balls and sticks) and π (lined p orbitals) systems of a hypothetical $C_{12}H_{24}$ molecule form two peprendicular Möbius strips.

IV. THE MÖBIUS MODEL BEYOND THE $R \gg L$ APPROXIMATION

So far, R was considered sufficiently larger than L so $r \approx R$. Lifting this constraint, $\hat{L}_z$ ceases to provide a good quantum number, and the $e^{im\phi}$ functions can no longer be used. However, the $\hat{P}_\phi$ operator, related to the C_2 axis, commutes with the Hamiltonian, and thus $\cos(m\phi)$ and $\sin(m\phi)$ serve as an adequate "basis set" (m takes now only positive values). Moreover, the two sets (of sine and cosine) can be employed separately; the cosine set belongs to the A irreducible representation and the sine set to the B one (C_2 point group; see Fig. 1). Note also that the energy degeneracy claimed in Sec. III is no longer expected.

At first approximation, however, the lowest states with odd n and $m = 0,1$ have no ($m = 0$) and two nodes ($m = 1$) referring to ϕ: $\cos\phi$ nullifies at $\phi = \pi/2, 3\pi/2$ and $\sin\phi$ at $\phi = 0, \pi$. Similarly, for even n we have one and three nodes for $m = 1/2$ and $3/2$, respectively. To corroborate these claims, Hartree-Fock calculations were performed on a hypothetical $C_{12}H_{24}$ molecule with Möbius conformation (see Fig. 7). The basis set used is the minimal $1s/_{H}\ 2s1p/_{C}$ while geometric

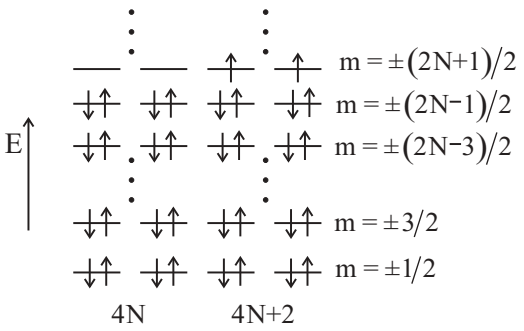

FIG. 8. Diagram of the first $2N$ energy levels [$|m| = \frac{1}{2} - \frac{2N+1}{2}$] of the particle in a Möbius surface with $n =$ even (π conjugated system), occupied with $4N$ and $4N + 2$ electrons. The energies of the levels are not in scale.

parameters are $R = 3.0$ Å and $L = 2.0$ Å ($r_{C-C} = 1.55$ Å, $r_{C-H} = 1.0$ Å). Calculations were performed using the MOLPRO suites of codes [14]. The resulting molecular orbitals are consistent with the present thoughts (see Fig. 9), confirming the proposed boundary conditions.

Next, a numerical solution of the general problem of a particle on a Möbius surface is presented, which is a variation of that used to simulate hindered internal rotations [15]. A grid of (s_p, ϕ_q) points is created so $s_p = p\delta$ and $\phi_q = q\epsilon$, with $p = -n_s, \ldots, -1, 0, 1, \ldots, n_s$ and $q = 0, 1, \ldots, n_\phi$, where δ, ϵ are the intervals between two successive grid points with ϕ, s constant, respectively. Since $-L/2 \leqslant s \leqslant L/2$ and $0 \leqslant \phi \leqslant 2\pi$, then $\delta = L/2n_s$ and $\epsilon = 2\pi/n_\phi$.

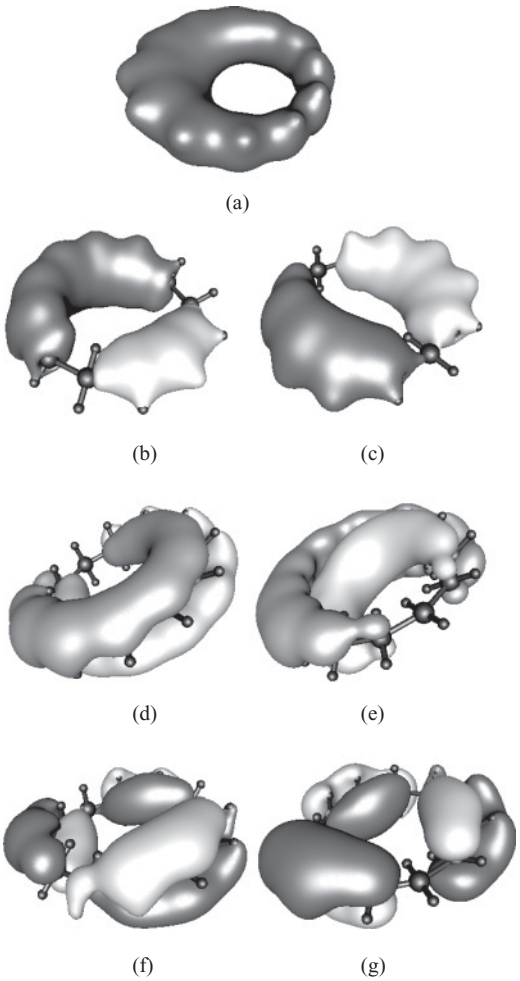

FIG. 9. Selected molecular orbitals of the Möbius-like $C_{12}H_{24}$ molecule. The positive part is depicted in gray and the negative part in white. (a) The first valence σ orbital of A symmetry ($n = 1$, $m = 0$, cosine case). (b) The second valence σ orbital of A symmetry ($n = 1$, $m = 1$, cosine case). (c) The first valence σ orbital of B symmetry ($n = 1$, $m = 1$, sine case). (d) The first π orbital of A symmetry ($n = 2$, $m = 1/2$, cosine case). (e) The first π orbital of B symmetry ($n = 2$, $m = 1/2$, sine case). (f) The second π orbital of A symmetry ($n = 2$, $m = 3/2$, cosine case). (g) The second π orbital of B symmetry ($n = 2$, $m = 3/2$, sine case).

Setting $\Psi(s_p, \phi_q)$ as $\Psi_{p,q}$, the first and second partial derivatives are approximated as follows:

$$\left(\frac{\partial\Psi}{\partial s}\right)_{s_p,\phi_q} = \frac{\Psi_{p+1,q} - \Psi_{p-1,q}}{2\delta} \tag{12}$$

$$\left(\frac{\partial\Psi}{\partial \phi}\right)_{s_p,\phi_q} = \frac{\Psi_{p,q+1} - \Psi_{p,q-1}}{2\epsilon} \tag{13}$$

$$\left(\frac{\partial^2\Psi}{\partial s^2}\right)_{s_p,\phi_q} = \frac{\Psi_{p+1,q} + \Psi_{p-1,q} - 2\Psi_{p,q}}{\delta^2} \tag{14}$$

$$\left(\frac{\partial^2\Psi}{\partial \phi^2}\right)_{s_p,\phi_q} = \frac{\Psi_{p,q+1} + \Psi_{p,q-1} - 2\Psi_{p,q}}{\epsilon^2} \tag{15}$$

Introducing them to the Schrödinger equation (5) [see also Eq. (A10)], we get

$$a_{p,q}\Psi_{p+1,q} + b_{p,q}\Psi_{p-1,q} + c_{p,q}\Psi_{p,q+1} + d_{p,q}\Psi_{p,q-1} + e_{p,q}\Psi_{p,q} = -\frac{2\mu E}{\hbar^2}\Psi_{p,q} \tag{16}$$

where

$$a_{p,q} = \frac{1}{\delta^2} + \frac{\cos(\phi_q/2)}{2r_{p,q}\delta} \tag{17}$$

$$b_{p,q} = \frac{1}{\delta^2} - \frac{\cos(\phi_q/2)}{2r_{p,q}\delta} \tag{18}$$

$$c_{p,q} = \frac{1}{r_{p,q}^2\epsilon^2} + \frac{s_p \sin(\phi_q/2)}{4r_{p,q}^3\epsilon} \tag{19}$$

$$d_{p,q} = \frac{1}{r_{p,q}^2\epsilon^2} - \frac{s_p \sin(\phi_q/2)}{4r_{p,q}^3\epsilon} \tag{20}$$

$$e_{p,q} = -2\left[\frac{1}{\delta^2} + \frac{1}{r_{p,q}^2\epsilon^2}\right] \tag{21}$$

and

$$r_{p,q} = R + s_p \cos(\phi_q/2). \tag{22}$$

We apply this equation for all points with $p = -n_s$ to n_s and $q = 1$ to n_ϕ; thus involving $\Psi_{p,q}$ values with $p = -(n_s + 1)$ to $(n_s + 1)$ and $q = 0$ to $(n_\phi + 1)$. After taking into consideration that $\Psi_{\pm n_s,q} = \Psi_{\pm(n_s+1),q} = 0$ for any q, and $\Psi_{p,0} = \Psi_{-p,n_\phi}$ or $\Psi_{p,n_\phi+1} = \Psi_{-p,1}$ for any p [boundary conditions of Eq. (9)], we finally involve only $\{\Psi_{p,q}\}_{p=-n_s+1,n_s-1}^{q=1,n_\phi}$ values. Consequently, the set of $M = (2n_s - 1)n_\phi$ equations can be condensed to the matrix form

$$A\Psi = \frac{2\mu E}{\hbar^2}\Psi, \tag{23}$$

where A is a sparse matrix containing the $a_{p,q}, b_{p,q}, c_{p,q}, d_{p,q}$, and $e_{p,q}$ values and Ψ is a column vector containing its M $\Psi_{p,q}$ components

$$\Psi = \begin{bmatrix} \Psi_{-n_s+1,1} \\ \cdots \\ \Psi_{-n_s+1,n_\phi} \\ \Psi_{-n_s+2,1} \\ \cdots \\ \Psi_{n_s-1,n_\phi} \end{bmatrix}. \tag{24}$$

TABLE I. Energy levels E (a.u.) of an electron confined to a Möbius strip with $R = 5.67$ a.u. and $L = 3.78$ a.u. The approximate energies $E_{n,m}$ (a.u.) as calculated from Eq. (8) are also given.

State(s)	E		$E_{n,m}$	n	m
1	0.343 249		0.345 371	1	0
2,3	0.359 271	0.359 366	0.360 924	1	±1
4,5	0.406 886	0.406 886	0.407 582	1	±2
6,7	0.485 931	0.485 931	0.485 345	1	±3
8,9	0.596 002	0.596 002	0.594 213	1	±4
10,11	0.736 518	0.736 518	0.734 187	1	±5
12,13	0.906 761	0.906 761	0.905 266	1	±6
14,15	1.105 908	1.105 908	1.107 450	1	±7
16,17	1.333 071	1.333 071	1.340 740	1	±8
18,19	1.382 400	1.384 558	1.385 373	2	±1/2
20,21	1.416 172	1.416 172	1.416 478	2	±3/2
22,23	1.481 483	1.481 483	1.478 689	2	±5/2
24,25	1.579 569	1.579 569	1.572 005	1	±9
26,27	1.587 348	1.587 348	1.605 134	2	±7/2
28,29	1.710 533	1.710 533	1.696 426	2	±9/2
30,31	1.867 863	1.867 863	1.851 952	2	±11/2
32,33	1.874 492	1.874 492	1.900 634	1	±10
34,35	2.071 547	2.071 547	2.038 584	2	±13/2

Diagonalizing the A matrix, we obtain the desired eigenvalues and eigenvectors. Actually more accurate approximations for the partial derivatives can be used, including $\Psi_{p-k,q}, \Psi_{p,q-k}$ with $k > 1$, and thus n_s, n_ϕ can be reduced considerably.

The previous methodology was applied to a Möbius surface resembling the $C_{12}H_{24}$ molecule [$R = 3.0$ Å or 5.67 a.u., $L = 2.0$ Å or 3.78 a.u., $\mu = 1.0$ a.u., $n_s = 1500$, $n_\phi = 100$, maximum k for s derivatives was set to 1 and for ϕ derivatives to 3]. Diagonalization was accomplished with MATLAB [16] and our numerical results are shown in Table I. Observe that the lowest energy levels, anticipated to be degenerate, differ in energy by some μE_h (see states 2, 3 and 18, 19 in Table I). The degeneracy, however, is recovered while m is increasing.

V. SYNOPSIS

Both the Hückel and the Möbius aromaticity have been demonstrated using the simplest possible models. Molecules of a ringlike conformation were simulated to a noninteracting system of electrons trapped in a cylinder, while Möbius-like molecules were simulated to an analogous system in a Möbius surface. The present study confirms the rules of $4N + 2$ and $4N$ electrons attributed to the Hückel and Möbius aromaticity, respectively. In addition, half-integer orbital angular momentum is predicted for a Möbius particle. Finally, a numerical method is suggested so the particle-in-a-Möbius-strip model can be solved. Compared to the ring model the double degeneracy in the Möbius model is practically retained. However, the contribution of the electron-electron repulsion and the nucleus-electron attraction of a real Möbius molecule have been ignored. Such many-body interactions are not expected to change the conclusions drawn. Although they will change the exact energy of the orbitals, there is no obvious reason for them to favor either of the degenerate orbitals, keeping the degeneracy present. This is exactly the case at least in the "real" benzene.

ACKNOWLEDGMENTS

The author is very grateful to Professor Aristides Mavridis for the fruitful discussions.

APPENDIX: THE LAPLACIAN OPERATOR IN THE MÖBIUS SPACE

In this appendix the Laplacian operator is calculated as a function of s and ϕ. The Cartesian coordinates x, y, and z are related to s,ϕ through the set of Eq. (4). The inverse transformation (s,ϕ as a function of x, y, and z) is shown below

$$\tan\phi = y/x$$
$$s = \{z^2 + [(x^2+y^2)^{1/2} - R]^2\}^{1/2}. \tag{A1}$$

The derivatives connecting the two sets of variables are [also using Eq. (4)]

$$\frac{\partial\phi}{\partial x} = \frac{\partial\phi}{\partial\tan\phi}\frac{\partial\tan\phi}{\partial x} = \cos^2\phi\left(-\frac{y}{x^2}\right) = -\frac{\sin\phi}{r}. \tag{A2}$$

Likewise

$$\frac{\partial\phi}{\partial y} = \frac{\cos\phi}{r} \tag{A3}$$

$$\frac{\partial\phi}{\partial z} = 0 \tag{A4}$$

$$\frac{\partial s}{\partial x} = \cos(\phi/2)\cos\phi \tag{A5}$$

$$\frac{\partial s}{\partial y} = \cos(\phi/2)\sin\phi \tag{A6}$$

$$\frac{\partial s}{\partial z} = \pm\sin(\phi/2). \tag{A7}$$

The $\pm$ symbol covers both enantiomers.

Setting $\vec{u} = (u_1,u_2,u_3) \equiv (x,y,z)$ and $\vec{v} = (v_1,v_2) \equiv (s,\phi)$ the Laplacian becomes (k runs from 1 to 3 and i,j from 1 to 2)

$$\begin{aligned}
\nabla^2 &= \sum_k \frac{\partial^2}{\partial u_k^2} \\
&= \sum_k \frac{\partial}{\partial u_k}\frac{\partial}{\partial u_k} = \sum_k \left(\sum_i \frac{\partial v_i}{\partial u_k}\frac{\partial}{\partial v_i}\right)\left(\sum_j \frac{\partial v_j}{\partial u_k}\frac{\partial}{\partial v_j}\right) \\
&= \sum_k \sum_{i,j} \frac{\partial v_i}{\partial u_k}\frac{\partial}{\partial v_i}\left(\frac{\partial v_j}{\partial u_k}\frac{\partial}{\partial v_j}\right) \\
&= \sum_k \sum_{i,j} \frac{\partial v_i}{\partial u_k}\frac{\partial}{\partial v_i}\left(\frac{\partial v_j}{\partial u_k}\right)\frac{\partial}{\partial v_j} + \sum_k \left[\sum_i \left(\frac{\partial v_i}{\partial u_k}\right)^2 \right. \\
&\quad \left. \times \frac{\partial^2}{\partial v_i^2} + 2\sum_{i,j>i} \frac{\partial v_i}{\partial u_k}\frac{\partial v_j}{\partial u_k}\frac{\partial^2}{\partial v_i \partial v_j}\right] \\
&= \sum_j \left[\sum_{i,k} \frac{\partial v_i}{\partial u_k}\frac{\partial}{\partial v_i}\left(\frac{\partial v_j}{\partial u_k}\right)\right]\frac{\partial}{\partial v_j} + \sum_i \left[\sum_k \left(\frac{\partial v_i}{\partial u_k}\right)^2\right] \\
&\quad \times \frac{\partial^2}{\partial v_i^2} + 2\sum_{i,j>i}\left[\sum_k \frac{\partial v_i}{\partial u_k}\frac{\partial v_j}{\partial u_k}\right]\frac{\partial^2}{\partial v_i \partial v_j}.
\end{aligned} \tag{A8}$$

For instance, the term accompanying $\partial^2/\partial s\partial\phi$ is

$$2\sum_k \frac{\partial\phi}{\partial u_k}\frac{\partial s}{\partial u_k} = 2\left[\frac{\partial\phi}{\partial x}\frac{\partial s}{\partial x} + \frac{\partial\phi}{\partial y}\frac{\partial s}{\partial y} + \frac{\partial\phi}{\partial z}\frac{\partial s}{\partial z}\right], \quad \text{(A9)}$$

which finally leads to 0, on using Eqs. (A2)–(A7).

In the long term, the Laplacian for both isomers is written as

$$\nabla^2 = \frac{\partial^2}{\partial s^2} + \frac{\cos(\phi/2)}{r}\frac{\partial}{\partial s} + \frac{1}{r^2}\frac{\partial^2}{\partial\phi^2} + \frac{s\sin(\phi/2)}{2r^3}\frac{\partial}{\partial\phi}. \quad \text{(A10)}$$

Recall that $r = R + s\cos(\phi/2)$ and thus

$$\frac{\partial r}{\partial s} = \cos(\phi/2) \quad \text{(A11)}$$

$$\frac{\partial(1/r)}{\partial\phi} = -\frac{1}{r^2}\frac{\partial r}{\partial\phi} = \frac{s\sin(\phi/2)}{2r^2}, \quad \text{(A12)}$$

due to which the Laplacian adopts the compact form

$$\nabla^2 = \frac{1}{r}\frac{\partial}{\partial s}r\frac{\partial}{\partial s} + \frac{1}{r}\frac{\partial}{\partial\phi}\frac{1}{r}\frac{\partial}{\partial\phi}. \quad \text{(A13)}$$

[1] J. Clayden, N. Greeves, S. Warren, and P. Wothers, *Organic Chemistry* (Oxford University Press, New York, 2001).

[2] M. Glukhovtsev, J. Chem. Educ. **74**, 132 (1997).

[3] J. A. N. F. Gomes and R. B. Mallion, Chem. Rev. **101**, 1349 (2001).

[4] For a historical review and an amusing lining up of applications of the Möbius strip, see C. A. Pickover, *The Möbius Strip* (Thunder's Mouth Press, New York, 2006).

[5] See, for instance, H. S. Rzepa, Chem. Rev. **105**, 3697 (2005); R. Herges, *ibid.* **106**, 4820 (2006), and references therein.

[6] C. S. Wannere, H. S. Rzepa, B. C. Rinderspacher, A. Paul, C. S. M. Allan, H. F. Schaefer, III, and P. v. R. Schleyer, J. Phys. Chem. A **113**, 11619 (2009).

[7] M. Stępień, L. Latos-Grażyński, N. Sprutta, P. Chwalisz, and L. Szterenberg, Angew. Chem. Int. Edn. **46**, 7869 (2007).

[8] R. Herges, Nature (London) **450**, 36 (2007).

[9] J. M. Lim, J.-Y. Shin, Y. Tanaka, S. Saito, A. Osuka, and D. Kim, J. Am. Chem. Soc. **132**, 3105 (2010).

[10] E. Heilbronner, Tetrahedron Lett. **5**, 1923 (1964).

[11] P. W. Fowler, E. Steiner, R. W. A. Havenith, and L. W. Jenneskens, Magn. Reson. Chem. **42**, S68 (2004), and references therein.

[12] J. Gravesen and M. Willatzen, Phys. Rev. A **72**, 032108 (2005).

[13] E. W. Weisstein, "Möbius Strip." From MathWorld—A Wolfram Web Resource, [http://mathworld.wolfram.com/MoebiusStrip.html], and references therein.

[14] MOLPRO, version 2006.1, a package of *ab initio* programs, H.-J. Werner *et al.*, see[http://www.molpro.net.]

[15] G. Ercolani, J. Chem. Educ. **77**, 1495 (2000).

[16] MATLAB, version 7.8 (R2009A), available at [www.mathworks.com] (March 2010).